The Shot CH1 domain recognises a distinct form of F-actin during *Drosophila* oocyte determination

D. Nashchekin[1*], I. Squires[1†], A. Prokop[2] and D. St Johnston[1*]

Affiliations:

[1]The Gurdon Institute and the Department of Genetics, University of Cambridge; Tennis Court Road, Cambridge, United Kingdom.

[2]The University of Manchester, Manchester Academic Health Science Centre, Faculty of Biology, Medicine and Health, School of Biology, Manchester, United Kingdom.

*Corresponding author. Email: d.nashchekin@gurdon.cam.ac.uk d.stjohnston@gurdon.cam.ac.uk,

[†]Present address: Biosciences Institute, Newcastle University, Newcastle upon Tyne, United Kingdom.

Abstract

As in mammals, only one cell in a *Drosophila* multicellular female germline cyst is specified as an oocyte. The symmetry-breaking cue for oocyte selection is provided by the fusome, a tubular structure connecting all cells in the cyst. The *Drosophila* spectraplakin Shot localises to the fusome and translates its asymmetry into a polarised microtubule network that is essential for oocyte specification, but how Shot recognises the fusome is unclear. Here we demonstrate that Shot's actin-binding domain (ABD) is necessary and sufficient to localise Shot to the fusome and mediates Shot function in oocyte specification together with the microtubule-binding domains. The calponin homology domain 1 (CH1) of Shot's ABD recognises fusomal F-actin and requires CH2 to distinguish it from other forms of F-actin in the cyst. By contrast, the ABDs of Utrophin, Fimbrin, Filamin, Lifeact and F-tractin do not recognise fusomal F-actin. We therefore propose that Shot propagates fusome asymmetry by recognising a specific conformational state of F-actin on the fusome.

Introduction

Both male and female gametes differentiate inside cysts of interconnected germ cells. Whereas all male cells in the cyst become sperm, only one or few of the female germ cells are specified to become oocytes in most animals (Lu et al., 2017, Pepling and Spradling, 1998, Lei and Spradling, 2013). Since cells in the female germline cyst share cytoplasm through intercellular bridges, there must be specific mechanisms to select the future oocyte. In *Drosophila*, a polarised microtubule (MT) network extends throughout the cyst and directs the dynein-dependent transport of oocyte fate determinants into one cell (Theurkauf et al., 1993; Li et al., 1994). A similar mechanism could also be involved in oocyte specification in the mouse (Lei and Spradling, 2016; Niu and Spradling, 2022).

In *Drosophila*, cyst formation and oocyte specification occur in the germarium at the anterior of the fly ovary (Fig. 1A). Oocyte determination starts when a germline stem cell divides asymmetrically to produce a cyst progenitor, a cystoblast, that goes through 4 rounds of incomplete division to produce a cyst of 16 cells connected by intercellular bridges called ring canals (de Cuevas et al., 1997). The cystoblast contains a spherical structure inherited from the stem cell called the spectrosome, which contains endoplasmic reticulum, spectrins and actin-binding proteins (Lighthouse et al., 2008). At each subsequent division, new spectrosomal material forms in the ring canal connecting the two daughter cells and this fuses with the pre-existing spectrosome to form the fusome, which becomes a branched structure extending into all 16 cells of the cyst (Lin et al., 1994; De Cuevas and Spradling, 1998). Because one cell inherits the original spectrosome/fusome from the cystoblast, this cell contains more fusomal material than the others and this ultimately specifies it as the pro-oocyte (Lin and Spradling, 1995; De Cuevas and Spradling, 1998).

The first step in the translation of fusome asymmetry into oocyte specification is the recruitment of the *Drosophila* spectraplakin, Shot (Roper and Brown, 2004; Nashchekin et al., 2021). Shot in turn recruits the MT minus end-binding protein Patronin (CAMSAP in mammals) to the fusome, where Patronin stabilises microtubule minus ends (Goodwin and Vale, 2010; Jiang et al., 2014; Nashchekin et al., 2021). The slight excess of Patronin in the future oocyte is then amplified by the

71 dynein-dependent transport of Patronin and microtubule minus ends along the
72 stabilised microtubules into this cell, leading to the formation of non-centrosomal
73 microtubule-organising centres (ncMTOCs) in the future oocyte. Finally, these
74 ncMTOCs nucleate a polarised MT network that directs the transport of oocyte
75 determinants into this cell (Grieder et al., 2000; Bolívar et al., 2001; Nashchekin et
76 al., 2021) (Fig. 1B).
77
78 The spectraplakin Shot belongs to a conserved family of actin-microtubule
79 crosslinkers that includes human Dystonin and MACF1/ACF7, which play important
80 roles in cytoskeletal organisation during neurogenesis and in epithelia (Lee and
81 Kolodziej, 2002; Voelzmann et al., 2017; Dogterom and Koenderink, 2018).
82 Spectraplakins are characterised by an N-terminal actin-binding domain (ABD), a
83 central long rod domain consisting of plakin and spectrin repeats and a C-terminal
84 MT-binding module (Fig. 1C). The ABD of spektraplakins consists of tandem
85 calponin homology domains, CH1 and CH2 and the MT-binding module is composed
86 of the MT lattice-binding GAS2 domain and an unstructured C-terminal domain
87 containing two SxIP motifs that interact with the MT plus end-binding protein EB1
88 (Sun et al., 2001; Honnappa et al., 2009; Applewhite et al., 2010; Alves-Silva et al.,
89 2012). Although Shot transmits fusome asymmetry to Patronin localisation and the
90 formation of the polarised MT network that specifies the oocyte, how Shot
91 recognises the fusome is not known. Previous work suggested that the Shot ABD is
92 not involved (Roper and Brown, 2004). Here we show, however, that both the actin
93 and MT-binding domains are required for oocyte specification, consistent with Shot's
94 role in organising the polarised microtubule network. The Shot ABD is necessary and
95 sufficient for localisation to the fusome and recognises a form of F-actin that differs
96 from other F-actin networks in the cyst.
97
98 **Results and Discussion**
99 **The Shot actin-binding domain localises to the fusome**
100 To determine which Shot domain(s) direct its localisation to the fusome, we
101 expressed a mini-version of Shot lacking the central rod domain, Shot-NC (Figure
102 1C). It has been previously shown that the NC version of ACF7 (a mammalian Shot
103 homologue) partially substitutes for ACF7 function in cells (Wu et al., 2008). Like
104 endogenous Shot and the full-length Shot transgene (Fig. 1D and 1E, respectively),

105 Shot-NC localised to the fusome, which is marked by a-spectrin (Fig. 1F and S1A).
106 Thus, the fusome-binding activity of Shot resides in either its N- or C-terminal
107 domains and the rod domain is dispensable for fusome localisation. Expression of
108 the N- or C-terminal domains alone showed that Shot-N binds to the fusome in wild
109 type and *shot* mutant cysts (Fig. 1G and Fig. 2C, respectively), whereas Shot-C
110 forms cytoplasmic foci and accumulates in one cell of the cyst in wild-type (Fig. S1A
111 and S1B) but not in *shot* mutant cysts (Fig. S1D), a pattern previously described for
112 EB1 (Nashchekin et al., 2021). Live imaging of Shot-C-YFP in the germarium
113 revealed that it forms EB1-like comets (Video1) suggesting that the C-terminal
114 domain of Shot associates with MT plus ends, and that the MT lattice-binding GAS2
115 domain is in an inhibited conformation, as shown for the mammalian Shot
116 homologue, Dystonin, in Cos-7 cells (Kapur et al., 2012). Nevertheless, we decided
117 to test whether the GAS2 domain has the potential to bind the fusome by expressing
118 a portion of the Shot C-terminal domain containing the EF hand and the GAS2
119 domain that has strong MT binding activity (Maybeck and Roper, 2009). EF-GAS2-
120 GFP localised to the fusome in the presence of endogenous Shot (Fig. S1A and
121 S1B) but failed to do so in *shot* mutant cysts (Fig. S1C and S1D). Fusome-
122 associated MTs are largely lost in the absence of Shot, indicating that EF-GAS2-
123 GFP localises to the fusome by binding to Shot-dependent MT (Roper and Brown,
124 2004). The GAS2 domain therefore cannot be responsible for the initial recruitment
125 of Shot to the fusome.
126
127 From our results so far, we speculated that Shot recruitment to the fusome requires
128 the Shot N-terminal region containing the two Calponin homology domains that
129 constitute the ABD. We therefore expressed a construct containing just the ABD of
130 Shot fused to GFP and confirmed its localisation to the fusome (Fig. 1H and S1A). In
131 contrast, full-length Shot lacking the ABD ($Shot^{\Delta ABD}$) showed only a residual fusome
132 localisation (Fig. 1I and S1A) that disappeared in the absence of endogenous Shot
133 (Fig. S1D) like Shot C and Shot EF-GAS. Thus, the ABD of Shot is both necessary
134 and sufficient for fusome localisation, presumably by interacting with fusome-
135 associated F-actin.
136

137 **The actin- and MT-binding domains of Shot are required for the oocyte**
138 **specification**
139
140 The oocyte is not specified in the absence of Shot, leading to the formation of a 16
141 nurse cell follicle, but which domains of Shot are required for oocyte specification is
142 not known (Roper and Brown, 2004). The cytoplasmic polyadenylation element
143 binding factor oo18 RNA-binding protein (Orb) is an early marker for oocyte
144 specification that becomes concentrated in the oocyte in regions 2b and 3 in wild-
145 type germaria but it is uniformly distributed in *shot* null mutant cysts (Lantz et al.,
146 1994; Roper and Brown, 2004) (Fig. 2A and 2B). To determine whether the presence
147 of the Shot actin- or MT-binding domains are sufficient for oocyte specification, we
148 expressed Shot-N, Shot-C, Shot-NC and Shot-EF-GAS2 in *shot* null mutant cysts
149 (Fig. 2C-D and S1D). Although Shot-N bound to the fusome in the absence of
150 endogenous Shot, it did not rescue Orb localisation and oocyte determination (Fig.
151 2C). Neither Shot-C or Shot-EF-GAS2 localised to the fusome or rescued oocyte
152 specification in *shot* mutants (Fig. Fig. S1C-D). However, Shot-NC expression
153 restored oocyte specification in the absence of full length Shot (Fig. 2D). Thus, both
154 the ABD and MT-binding modules are necessary for Shot function during oocyte
155 determination, suggesting that Shot acts as an actin-microtubule cross-linker in this
156 context.
157
158 It has been previously reported that Shot's ABD is not required for oocyte
159 specification, since the oocyte is specified normally in cysts mutant for $shot^{kakp1}$, a P-
160 element insertion that is predicted to prevent the expression of CH1 domain-
161 containing Shot isoforms (Roper and Brown 2004). As shown above, however,
162 Shot's ABD is essential for the Shot localisation to the fusome and oocyte
163 determination. To resolve this contradiction, we tested the requirement for Shot's
164 CH1 and CH2 domains in oocyte specification by expressing $Shot^{\Delta ABD}$, $Shot^{\Delta ABD}$-
165 LifeAct, $Shot^{\Delta CH1}$ and $Shot^{\Delta CH2}$ in *shot* mutant cysts (Fig. 2E-F and S1D). Shot
166 truncations lacking the CH1 domain did not rescue oocyte specification, nor did
167 substituting the Shot ABD with the actin-binding activity of LiveAct (Fig. 2E and
168 S1D). Only *shot* mutant cysts expressing $Shot^{\Delta CH2}$ maintained Orb localisation and
169 specified the oocyte (Fig. 2F). Thus, the CH1 domain of Shot's ABD is essential for
170 the oocyte specification. Since the $shot^{kakp1}$ mutant does not affect oocyte

171 determination, we assume that this P-element insertion does not disrupt the
172 expression of CH1-containing Shot isoforms in the germ line, although it does so in
173 somatic tissues (Roper and Brown 2004).
174
175 Previously, it has been proposed that Shot binds the fusome with an unidentified
176 domain and uses its GAS2 domain to bind and stabilise MT (Roper and Brown,
177 2004). Based on our results we propose an alternative model for Shot function in
178 oocyte determination where it works as a classical actin-MT cytolinker by recognising
179 fusomal F-actin with its ABD and using its C-terminal domain to attach MT to the
180 fusome. Which part of the MT module is involved in this process is an open question.
181 On the one hand, Shot-EF-GAS2 can recognise fusomal MT. On the other hand,
182 expression of the whole Shot C-terminal domain showed that the GAS2 domain is
183 not exposed and Shot C interacts only with MT plus ends through its EB1-binding
184 motifs. Thus, Shot may guide the growth of MT plus ends along the fusome in a
185 similar manner to that described for ACF7 in migrating cells (Kodama et al., 2003;
186 Wu et al., 2008). The role of Shot in stabilising MT on the fusome could also be
187 indirect, since we recently showed that Shot is required for the fusome localisation of
188 the MT minus-end stabilising protein Patronin/CAMSAP (Nashchekin et al., 2021).
189 Moreover, fusome-associated MT are unstable in *patronin* mutant cysts even though
190 Shot is still present. How Shot's C-terminus recruits microtubules to the fusome will
191 therefore require further study.
192
193 **Shot recognises a distinctive form of F-actin on the fusome**
194 Several actin-binding proteins have been identified as components of the fusome,
195 including b-spectrin, Hts/Adducin, Tropomodulin and Shot (De Cuevas et al., 1996;
196 Lin et al., 1994; Lighthouse et al., 2008; Roper and Brown, 2004). However, actin
197 has never been detected in the fusome and Phalloidin does not label the fusome,
198 staining only the ring canals and the cell cortex (Warn et al., 1985 and Fig. 1D-I). In
199 contrast, Actin-GFP weakly localises to the fusome, raising the possibility that the
200 absence of Phalloidin staining might be misleading (Fig. S2A). We therefore tested
201 for the presence of endogenous actin in the fusome by performing antibody stainings
202 for actin using various fixation methods. Only a combination of heat fixation followed
203 by post-fixation with formaldehyde produced convincing fusomal actin staining (Fig.

204 3A). As a control we used *hts* mutant cysts (Fig. S2B), which lack the fusome (Lin et
205 al., 1994), and confirmed that fusome-like actin staining was absent. We conclude
206 that the fusome does contain F-actin, but not in a form that can be detected by
207 Phalloidin. Since the Phalloidin-actin interaction is sensitive to the structure of F-actin
208 filaments (McGough et al., 1997), fusomal F-actin may exist in a distinct
209 conformation that can be bound by the Shot ABD but not by Phalloidin.
210
211 Both b-Spectrin and Shot are members of a large family of actin-binding proteins
212 with ABDs formed by tandem CH domains (Korenbaum and Rivero, 2002; Yin et al.,
213 2020) (Fig. S2C). To test whether other CH domain proteins recognise fusomal F-
214 actin, we analysed the distribution of over-expressed Utrophin ABD and
215 endogenously-tagged Filamin and Fimbrin. None of these CH domain proteins
216 recognised fusomal F-actin and they mainly concentrated at the ring canals in fixed
217 and live samples (Fig. 3B-D and S2D, respectively). F-tractin, LifeAct and SiR-actin
218 are other commonly used F-actin markers (Melak et al., 2017), recognising a variety
219 of F-actin structures (Riedl et al., 2008; Schell et al., 2001; Belin et al., 2014;
220 Spracklen et al., 2014; D'Este et al., 2015). Neither F-tractin or LifeAct localised to
221 the fusome, mainly localising to the cell cortex and ring canals (Fig. 3E-F and S2D).
222 Moreover, substituting Shot's ABD with the LifeAct sequence (Shot$^{\Delta ABD}$-LifeAct) did
223 not restore fusome recognition to full-length Shot (Fig. 3G and S1A). On the other
224 hand, SiR-actin weakly localised to the fusome (Fig. 3H). Thus, fusomal F-actin has
225 a distinctive conformation that is only recognised by a subset of actin-binding
226 proteins/reagents. The Shot ABD must therefore have structural features that allow it
227 to bind preferentially to fusomal F-actin and to distinguish it from other F-actin
228 structures in the cyst. This does not preclude the Shot ABD binding to other forms of
229 F-actin, since Shot re-localises to the cell cortex and ring canals in *hts* and *a-*
230 *spectrin* mutant cysts that lack the fusome (Lin and Spradling, 1995; De Cuevas et
231 al., 1996) (Fig. S3). Shot also binds to actin filaments at the ring canals at the later
232 stages of oogenesis when the fusome is disassembled (Lu et al., 2021).
233
234 The spatial arrangement of tandem CH1 and CH2 domains can regulate their actin
235 binding activity, as the CH2 domain can sterically block some of the actin binding
236 surfaces on the CH1 domain (Bañuelos et al., 1998; Galkin et al., 2010; Iwamoto et

al., 2018). It has been proposed that phosphorylation of a conserved Tyr located at the end of the CH2 domain facilitates the formation of an “open” conformation of the ACF7 ABD and enhances F-actin binding (Yue et al., 2016, Fig. 1C). To test whether Shot binding to the fusome is regulated by Tyr phosphorylation, we expressed Shot ABDs containing phosphomimetic and non-phosphorylatable versions of Tyr364 (ABD Y364D and ABD Y364F, respectively). Whereas ABD Y364F only bound to fusomal F-actin (Fig. 4B), ABD Y364D bound to the fusome and ring canals in region 2a of the germarium and mostly relocalised to ring canals in region 2b (Fig. 4A). This suggests that shifting the equilibrium towards an open state of the CH domains alters the specificity of Shot’s ABD for different forms of F-actin, rather than working as a simple on/off switch.

To examine the role of CH2 in regulating the actin-binding properties of CH1, we compared the localisation of CH1 alone with that of the full ABD containing CH1 and CH2. Whereas CH1-CH2 exclusively localised to the fusome (Fig. 1H and 4C), CH1 alone recognised F-actin on the fusome and ring canals (Fig. 4D). Thus, removing the CH2 domain has the same effect as the Y364D mutation in making CH1's binding to F-actin more promiscuous. According to recent structural studies, CH1-CH2 binds to F-actin filaments in an open conformation, with CH1 sitting in the groove between subdomains 1 and 2 of an actin monomer and CH2 oriented away from the filament (Galkin et al., 2010; Iwamoto et al., 2018; Kumari et al., 2020). This implies that binding of CH1 to F-actin breaks multiple interactions between the CH1 and the CH2 (Galkin et al., 2010; Yue at al., 2016; Iwamoto et al., 2018; Harris et al., 2019; Kumari et al., 2020; Harris et al., 2020). We can envisage two models for how CH2 controls the specificity of CH1's actin binding. CH2 in the closed conformation of the ABD may itself bind weakly to the specific form of actin on the fusome and thereby increase the avidity of the initial interaction of CH1-CH2 with fusomal actin. This increased avidity would then ensure that the Shot ABD binds preferentially to fusomal F-actin, which therefore outcompetes other F-actin in the cyst for Shot binding. Alternatively, CH2 may mask some actin binding surfaces of CH1 in the "closed" conformation of the ABD, allowing the latter to bind fusomal actin with higher affinity than other forms of actin. In another words, the presence of CH2 may increase the affinity of the ABD for fusomal actin or decrease its affinity to other forms of actin.

271

272 Since isolated ABDs could behave differently from the full-length protein, we
273 introduced the Tyr364 mutations into Shot-NC and full-length Shot. Whereas the
274 Shot-NC Tyr364 mutants behave like the corresponding ABD mutants, the
275 localisation of the full-length Shot was not affected by the Y364D mutation (Fig. 4E,
276 4F and S2E). Thus, sequences in the rod domain somehow restore the specificity of
277 the Y364D ABD for fusomal actin. We also tested the role each CH domain in the
278 context of the full-length protein by analysing the localisation of full-length Shot
279 lacking CH1 ($Shot^{\Delta CH1}$) or CH2 ($Shot^{\Delta CH2}$). $Shot^{DCH2}$ localised to the fusome normally
280 (Fig. 4H and S1A), whereas deletion of CH1 abolished fusome binding, leading to
281 cytoplasmic localisation (Fig. 4G and S1A). The same pattern was observed in the
282 absence of the endogenous Shot (Fig. 2F and 2E, respectively). These results
283 indicate that the CH1 domain mediates Shot binding to the fusome and that it can
284 recognise a specific F-actin conformation that is invisible to several other CH-domain
285 proteins and actin-binding molecules. This result also implies that specific binding to
286 fusomal F-actin by Shot, which depends on CH2 in the isolated ABD, does not
287 require CH2 in the context of the full-length protein.
288

289 Structural studies on the interaction of CH domains with F-actin have revealed that
290 CH1 interacts with two adjacent actin monomers and is sensitive to the
291 torque/helicity of F-actin filaments (Hanein et al., 1998; Iwamoto et al., 2018; Kumari
292 et al., 2020; Harris et al., 2020). Changes in the helical twist of F-actin filaments can
293 be caused by mechanical tension, by interactions with actin-binding proteins (Harris
294 et al., 2018; Jégou and Romet-Lemonne, 2020; Harris et al., 2020), or by the
295 bending of F-actin filaments promoted by differences in the nucleotide states of actin
296 monomers (Reynolds et al., 2022; Oosterheert et al., 2022). It is therefore possible
297 that CH1 domains of different actin-binding proteins are predisposed to bind F-actin
298 filaments with specific helical twists, which could explain their distinct, but partly
299 overlapping localisation patterns (Washington and Knecht, 2008; Harris et al., 2020;
300 Jégou and Romet-Lemonne, 2021).
301

302 Although the Y367D mutation and the removal of CH2 lead to promiscuous binding
303 of the Shot ABD to both the fusome and other F-actin in the cyst, they have no effect

304 on the specific localisation of full-length Shot to the fusome. This indicates that some
305 region of the full-length protein can substitute for CH2 in the "closed" conformation of
306 the ABD. This is most likely part of the rod domain since the Y367D mutation still
307 causes promiscuous actin binding in the context of ShotNC (Fig. 4E). As proposed
308 for CH2 in the context of the ABD alone, this rescue by the rod domain could be due
309 to an interaction between the rod and CH1 that masks some actin binding surfaces
310 to reduce its affinity for nonfusomal actin. Since the rod is very long, it is also
311 possible that this effect is indirect and acts by allowing the intramolecular interaction
312 between the C-terminal EF hands and CH1 to achieve the same effect (Applewhite
313 et al., 2013). Alternatively, the rod domain could increase the avidity of Shot's
314 interaction with the fusome by binding to some other fusomal component. Indeed,
315 Shot has been proposed to bind to a-Spectrin, which is enriched on the fusome
316 (Khanal et al., 2016; Lin et al., 1994; De Cuevas and Spradling, 1998). Since full-
317 length Shot^{DABD} does not localise to the fusome, the rod domain is unlikely function
318 as a strong fusome-binding domain itself, but may contribute to avidity in a similar
319 way to that proposed above for CH2.
320
321 Our evidence suggests that fusome asymmetry is propagated to MT organisation in
322 the *Drosophila* female germline cyst by the formation of a distinct type of F-actin on
323 the fusome, which then recruits the spectraplakin Shot. How fusomal F-actin is
324 formed and the structural basis for its recognition by actin-binding proteins remain to
325 be determined. Considering that Shot is a conserved actin binding protein, it is
326 possible that a similar mechanism is used in other contexts where F-actin filaments
327 in a specific mechanical state are recognised by only a subset of actin-binding
328 proteins.
329

330 **Material and methods**
331
332 **Drosophila stocks.** The following previously described *Drosophila melanogaster*
333 mutant alleles and transgenic lines were used: FRTG13 *shot*^{3} (Roper and Brown,
334 2004), *hts*^{1} and *hts*^{01103} (Yue and Spradling, 1992), *a-spectrin*$^{e2-26}$ (Hülsmeier et al.,
335 2007), UAS-GFP-Actin42A (Roper et al., 2005), UAS-GFP-Shot EF-GAS2 (Maybeck
336 and Roper, 2009); UAS-Shot$^{\Delta ABD}$-GFP, UAS-Shot$^{\Delta CH1}$-GFP, UAS-Shot$^{\Delta CH2}$-GFP and
337 UAS-Shot$^{\Delta ABD}$-LifeAct-GFP (Qu et al., 2022), Shot-YFP (Nashchekin et al., 2016),
338 UAS-F-tractin-tdTomato (Spracklen et al., 2014),Filamin-GFP trap line (gift from K.
339 Röper, MRC-LMB, UK), Fimbrin-YFP (Cambridge Protein Trap Insertion line 100066,
340 (Lowe et al., 2014), sqh>Utrophin ABD-GFP (Rauzi et al., 2010). UAS-Shot-GFP,
341 UAS-ShotY364F-GFP, UAS-ShotY364D-GFP, UAS-Shot-NC-YFP, UAS-Shot-
342 NCY364D-YFP, UAS-Shot-NCY364F-YFP, UAS-Shot-N-YFP, UAS-Shot-C-YFP,
343 UAS-GFP-Shot ABD, UAS-GFP-Shot ABDY364F, UAS-GFP-Shot ABDY364D, UAS-
344 LifeAct-RFP were generated for this study.
345
346 ***Drosophila* genetics.** Germline clones of *shot*^{3} *and a-spectrin*$^{e2-26}$ were induced by
347 incubating larvae at 37° for two hours per day over a period of three days. Clones
348 were generated with FRT G13 nlsRFP and FRT 2A nlsRFP, (Bloomington Stock
349 Center) using the heat shock Flp/FRT system (Chou and Perrimon, 1992). Germline
350 expression of UAS transgenes was induced by nanos>Gal4. All transgenes were
351 expressed in a wild-type background unless otherwise specified.
352
353 **Molecular Biology.** To generate pUASP Shot-GFP, three fragments of the *shot* RE
354 cDNA were amplified from pUAST Shot-GFP (Lee and Kolodziej, 2002) and cloned
355 together with EGFP into the pUASPattb vector. pUASPattb-Shot-NC-YFP was
356 generated by PCR amplifying fragments from pUAST Shot-GFP corresponding to
357 the first 520 aa (Shot-N) and last 462 aa (Shot-C) of Shot PE, cloning them together
358 into pUASP-YFP-Cterm and then re-cloning into pUASPattb. pUASPattb-Shot-N-
359 YFP and pUASPattb-Shot-C-YFP were generated by amplifying Shot-N or Shot-C
360 fragments from pUASPattb-Shot-NC-YFP and cloning them together with YFP into
361 pUASPattb. Shot ABD cDNA (corresponding to 146-368 aa of Shot PE) was
362 amplified from pUASPattb-Shot-NC-YFP and cloned together with EGFP into
363 pUASP-attb to generate pUASP-attb GFP-Shot ABD. The Q5 Site-Directed

364 Mutagenesis Kit (New England BioLabs) was used to generate pUASPattb-GFP-
365 Shot ABDY364F, pUASPattb-GFP-Shot ABDY364D, pUASPattb-Shot-NCY364D-
366 YFP and pUASPattb-Shot-NCY364F-YFP. Shot-N with the Y364F or Y364D
367 mutations was amplified from pUASPattb-Shot-NCY364F or pUASPattb-Shot-
368 NCY364D, respectively, and cloned together with two fragments covering the rest of
369 Shot RE cDNA and EGFP into pUASP-attb to generate pUASPattb-ShotY364F-GFP
370 and pUASPattb-ShotY364D-GFP. pUASP-LifeAct-tagRFP was generated according
371 to Riedl et al (2008). NEBuilder HiFi DNA Assembly (New England BioLabs) was
372 used for most of the cloning. Primer sequences are available on request.

373 **Immunohistochemistry**. Ovaries were fixed for 20 min at room temperature in 4%
374 paraformaldehyde and 0.2% Tween in PBS. Ovaries were then blocked with 1%
375 BSA in PBS with 0.2% Tween for 1 hr at room temperature. Ovaries were incubated
376 with the primary antibody for 16 hr with 0.1% BSA in PBS with 0.2% Tween at 4C°
377 and for 4 hr with the secondary antibody at room temperature. For detection of
378 fusomal F-actin, we used the heat fixation protocol described in Chen et al (2018)
379 with some modifications. Ovaries were dissected in PBS, fixed for 10 sec in hot
380 (95C°) 1xTSS (0.03% Triton X-100, 4 g/L NaCl), post-fixed in 8% paraformaldehyde
381 and 0.1% Triton X-100 in PBS for 10 min at room temperature and then treated as
382 above. We used the following primary antibodies: guinea pig anti-Shot at 1:1000
383 (Nashchekin et al., 2016), mouse anti-Orb at 1:10 (DSHB Hybridoma Products 4H8
384 and 6H4. Deposited to the DSHB by Schedl, P), mouse anti-a-Spectrin at 1:200
385 (DSHB Hybridoma Product 3A9. Deposited to the DSHB by Branton, D. / Dubreuil,
386 R.), mouse anti-Actin at 1:200 (clone AC-40, Merck), rabbit anti-b-spectrin at 1:200
387 (Byers et al., 1989), SiR-actin (1:100, Spirochrome). Secondary antibodies
388 conjugated with Alexa fluor dyes (Thermo Fisher Scientific) were used at 1:1000.

389 **Imaging.** Fixed preparations were imaged using a Leica SP8 (63x/1.4 HC PL Apo
390 CS Oil) confocal microscope. Germaria were imaged by collecting 10–15 z sections
391 spaced 0.5 µm apart. For live imaging, ovaries were dissected and imaged in
392 Voltalef oil 10S (VWR International) on a Leica SP5 confocal microscope (63x/1.4
393 HCX PL Apo CS Oil) or on an Olympus IX81 inverted microscope with a Yokogawa
394 CSU22 spinning disk confocal imaging system (100x/ 1.3 NA Oil UPlanSApo).
395 Images were collected with Leica LAS AF software or MetaMorph and processed

396 using ImageJ. The images are projections of several z sections.

397 **Reproducibility of experiments and statistical analyses.** Images are
398 representative examples from at least three independent repeats for each
399 experiment. The number of *shot*^{3} mutant cysts (region 2b to 3) with restored Orb
400 localisation after the expression of a rescue transgene were as follows: Figure 2A
401 wild type cysts (50/50), Figure 2B *shot*^{3} mutant cysts without a transgene (0/30),
402 Figure 2C Shot N (0/21), Figure S1D Shot-C (0/28), Figure S1D Shot EFGAS (0/18),
403 Figure 2D Shot NC (25/26), Figure S1D Shot$^{\Delta ABD}$ (0/14), Figure S1D Shot-LifeAct
404 (0/19), Figure 2E Shot$^{\Delta CH1}$ (0/16), Figure 2F Shot$^{\Delta CH2}$ (21/21). The number of cysts
405 analysed to determine the localisation of various Shot transgenes and actin-binding
406 reagents is summarised in Table S1. The chi-square test was used to test whether
407 values were significantly different between wild type and *shot*^{3} mutant cysts. The
408 Mann-Whitney t-test was used to determine significance when measuring the co-
409 localisation of Shot transgenes and fusome. A level of $p < 0.01$ was considered to be
410 statistically significant. No statistical methods were used to predetermine sample
411 size, the experiments were not randomized, and the investigators were not blinded to
412 allocation during experiments and outcome assessment.

413 **Supplemental material**
414 Figures S1-S3, Video 1 and Table S1.
415
416

417 **Acknowledgements**

418 We are grateful to Jean-René Huynh, Christian Klämbt, Thomas Lecuit, Katja Röper
419 and the Bloomington Drosophila Stock Center (NIH P40OD018537) for fly stocks,
420 the Gurdon Institute Imaging Facility for assistance with microscopy, John Overton
421 for technical assistance in making transgenic flies. We thank Jia Chen for help with
422 heat fixation.

423 Funding**:** Wellcome Principal Research Fellowship 080007 and 207496 (DStJ),
424 Wellcome core support 092096 and 203144 (DStJ), Cancer Research UK core
425 support A14492 and A24823 (DStJ), BBSRC grant BB/R001618/1 (DStJ, DN, IS).
426

References

Alves-Silva, J., N. Sanchez-Soriano, R. Beaven, M. Klein, J. Parkin, T.H. Millard, H.J. Bellen, K.J.T. Venken, C. Ballestrem, R.A. Kammerer, and A. Prokop. 2012. Spectraplakins Promote Microtubule-Mediated Axonal Growth by Functioning As Structural Microtubule-Associated Proteins and EB1-Dependent +TIPs (Tip Interacting Proteins). *Journal of Neuroscience*. 32:9143–9158. doi:10.1523/JNEUROSCI.0416-12.2012.

Applewhite, D.A., K.D. Grode, D. Keller, A.D. Zadeh, K.C. Slep, and S.L. Rogers. 2010. The Spectraplakin Short Stop Is an Actin-Microtubule Cross-Linker That Contributes to Organization of the Microtubule Network. *Mol Biol Cell*. 21:1714–1724. doi:10.1091/mbc.E10-01-0011.

Applewhite, D.A., K.D. Grode, M.C. Duncan, and S.L. Rogers. 2013. The actin-microtubule cross-linking activity of Drosophila Short stop is regulated by intramolecular inhibition. *Mol Biol Cell*. 24:2885–2893. doi:10.1091/mbc.E12-11-0798.

Bañuelos, S., M. Saraste, and K.D. Carugo. 1998. Structural comparisons of calponin homology domains: Implications for actin binding. *Structure*. 6:1419–1431. doi:10.1016/S0969-2126(98)00141-5.

Belin, B.J., L.M. Goins, and R.D. Mullins. 2014. Comparative analysis of tools for live cell imaging of actin network architecture. *Bioarchitecture*. 4:189–202. doi:10.1080/19490992.2014.1047714.

Bolívar, J., J.R. Huynh, H. López-Schier, C. González, D. St Johnston, and A. González-Reyes. 2001. Centrosome migration into the Drosophila oocyte is independent of BicD and egl, and of the organisation of the microtubule cytoskeleton. *Development*. 128:1889–1897.

Bolte S, Cordelieres FP. 2006. A guided tour into subcellular colocalization analysis in light microscopy. J Microsc. 224:213-32.

Byers, T.J., A. Husain-Chishti, R.R. Dubreuil, D. Branton, and L.S. Goldstein. 1989. Sequence similarity of the amino-terminal domain of Drosophila beta spectrin to alpha actinin and dystrophin. *Journal of Cell Biology*. 109:1633–1641. doi:10.1083/jcb.109.4.1633.

Chou, T.B., and N. Perrimon. 1992. Use of a yeast site-specific recombinase to produce female germline chimeras in Drosophila. *Genetics*. 131:643–653.

J. Chen, A.C. Sayadian, N. Lowe, H.E. Lovegrove, D. St Johnston, An alternative mode of epithelial polarity in the *Drosophila* midgut, Plos Biol. 16 (2018), e3000041.

De Cuevas, M., and A.C. Spradling. 1998. Morphogenesis of the Drosophila fusome and its implications for oocyte specification. *Development*. 125:2781–2789.

465 De Cuevas, M., J.K. Lee, and A.C. Spradling. 1996. α-spectrin is required for
466 germline cell division and differentiation in the Drosophila ovary. *Development*.
467 122:3959–3968.

468 de Cuevas, M., M.A. Lilly, and A.C. Spradling. 1997. Germline cyst formation in
469 Drosophila. *Annual Review of Genetics*. 31:405–428.
470 doi:10.1146/annurev.genet.31.1.405.

471 D'Este, E., Kamin, D., Gö ttfert, F., El-Hady, A. and Hell, S. W. (2015). STED
472 nanoscopy reveals the ubiquity of subcortical cytoskeleton periodicity in living
473 neurons. Cell Rep. 10, 1246-1251.

474 Dogterom, M., and G.H. Koenderink. 2018. Actin–microtubule crosstalk in cell
475 biology. *Nature Reviews Molecular Cell Biology 2018 19:5*. 13:1.
476 doi:10.1038/s41580-018-0067-1.

477 Galkin, V.E., A. Orlova, A. Salmazo, K. Djinovic-Carugo, and E.H. Egelman. 2010.
478 Opening of tandem calponin homology domains regulates their affinity for F-
479 actin. *Nat Struct Mol Biol*. 17:614–616. doi:10.1038/nsmb.1789.

480 Goodwin, S.S., and R.D. Vale. 2010. Patronin Regulates the Microtubule Network by
481 Protecting Microtubule Minus Ends. *Cell*. 143:263–274.
482 doi:10.1016/j.cell.2010.09.022.

483 Grieder, N.C., M. de Cuevas, and A.C. Spradling. 2000. The fusome organizes the
484 microtubule network during oocyte differentiation in Drosophila. *Development*.
485 127:4253–4264.

486 Hanein, D., N. Volkmann, S. Goldsmith, A.M. Michon, W. Lehman, R. Craig, D.
487 DeRosier, S. Almo, and P. Matsudaira. 1998. An atomic model of fimbrin binding
488 to F-actin and its implications for filament crosslinking and regulation. *Nat Struct*
489 *Biol*. 5:787–792. doi:10.1038/1828.

490 Harris, A.R., P. Jreij, and D.A. Fletcher. 2018. Mechanotransduction by the Actin
491 Cytoskeleton: Converting Mechanical Stimuli into Biochemical Signals. *Annual*
492 *Review of Biophysics*. 47:617–631. doi:10.1146/annurev-biophys-070816-
493 033547

494 Harris, A.R., P. Jreij, B. Belardi, A.M. Joffe, A.R. Bausch, and D.A. Fletcher. 2020.
495 Biased localization of actin binding proteins by actin filament conformation.
496 *Nature Communications*. 11:1–13. doi:10.1038/s41467-020-19768-9.

497 Honnappa, S., S.M. Gouveia, A. Weisbrich, F.F. Damberger, N.S. Bhavesh, H.
498 Jawhari, I. Grigoriev, F.J.A. van Rijssel, R.M. Buey, A. Lawera, I. Jelesarov, F.K.
499 Winkler, K. Wüthrich, A. Akhmanova, and M.O. Steinmetz. 2009. An EB1-binding
500 motif acts as a microtubule tip localization signal. *Cell*. 138:366–376.
501 doi:10.1016/j.cell.2009.04.065.

502 Hülsmeier, J., J. Pielage, C. Rickert, G.M. Technau, C. Klämbt, and T. Stork. 2007.
503 Distinct functions of alpha-Spectrin and beta-Spectrin during axonal pathfinding.
504 *Development*. 134:713–722. doi:10.1242/dev.02758.

505 Iwamoto, D.V., A. Huehn, B. Simon, C. Huet-Calderwood, M. Baldassarre, C.V.
506 Sindelar, and D.A. Calderwood. 2018. Structural basis of the filamin A actin-
507 binding domain interaction with F-actin. *Nat Struct Mol Biol*. 1–15.
508 doi:10.1038/s41594-018-0128-3.

509 Jégou, A., and G. Romet-Lemonne. 2020. The many implications of actin filament
510 helicity. *Seminars in Cell and Developmental Biology*. 102:65–72.
511 doi:10.1016/j.semcdb.2019.10.018.

512 Jégou, A., and G. Romet-Lemonne. 2021. Mechanically tuning actin filaments to
513 modulate the action of actin-binding proteins. *Current Opinion in Cell Biology*.
514 68:72–80. doi:10.1016/j.ceb.2020.09.002.

515 Jiang, K., S. Hua, R. Mohan, I. Grigoriev, K.W. Yau, Q. Liu, E.A. Katrukha, A.F.M.
516 Altelaar, A.J.R. Heck, C.C. Hoogenraad, and A. Akhmanova. 2014. Microtubule
517 minus-end stabilization by polymerization-driven CAMSAP deposition. *Dev Cell*.
518 28:295–309. doi:10.1016/j.devcel.2014.01.001.

519 Kapur, M., W. Wang, M.T. Maloney, I. Millan, V.F. Lundin, T.A. Tran, and Y. Yang.
520 2012. Calcium tips the balance: A microtubule plus end to lattice binding switch
521 operates in the carboxyl terminus of BPAG1n4. *EMBO Rep*. 13:1021–1029.
522 doi:10.1038/embor.2012.140.

523 Khanal, I., A. Elbediwy, M.D.C. Diaz de la Loza, G.C. Fletcher, and B.J. Thompson.
524 2016. Shot and Patronin polarise microtubules to direct membrane traffic and
525 biogenesis of microvilli in epithelia. *Journal of Cell Science*. 129:2651–2659.
526 doi:10.1242/jcs.189076.

527 Kodama, A., I. Karakesisoglou, E. Wong, A. Vaezi, and E. Fuchs. 2003. ACF7: An
528 essential integrator of microtubule dynamics. *Cell*. 115:343–354.
529 doi:10.1016/S0092-8674(03)00813-4.

530 Korenbaum, E., and F. Rivero. 2002. Calponin homology domains at a glance.
531 *Journal of Cell Science*. 115:3543–3545. doi:10.1242/jcs.00003.

532 Kumari, A., S. Kesarwani, M.G. Javoor, K.R. Vinothkumar, and M. Sirajuddin. 2020.
533 Structural insights into actin filament recognition by commonly used cellular actin
534 markers. *EMBO J*. 39:14869. doi:10.15252/embj.2019104006.

535 Lantz, V., J.S. Chang, J.I. Horabin, D. Bopp, and P. Schedl. 1994. The Drosophila
536 orb RNA-binding protein is required for the formation of the egg chamber and
537 establishment of polarity. *Genes Dev*. 8:598–613. doi:10.1101/gad.8.5.598.

538 Lee, S., and P.A. Kolodziej. 2002. Short Stop provides an essential link between F-
539 actin and microtubules during axon extension. *Development*. 129:1195–1204.

540 Lei, L., and A.C. Spradling. 2013. Mouse primordial germ cells produce cysts that
541 partially fragment prior to meiosis. *Development*. 140:2075–2081.
542 doi:10.1242/dev.093864.

543 Lei, L., and A.C. Spradling. 2016. Mouse oocytes differentiate through organelle
544 enrichment from sister cyst germ cells. *Science*. 352:95–99.
545 doi:10.1126/science.aad2156.

546 Li, M., M. McGrail, M. Serr, and T.S. Hays. 1994. Drosophila cytoplasmic dynein, a
547 microtubule motor that is asymmetrically localized in the oocyte. *The Journal of*
548 *Cell Biology*. 126:1475–1494. doi:10.1083/jcb.126.6.1475.

549 Lighthouse, D.V., M. Buszczak, and A.C. Spradling. 2008. New components of the
550 Drosophila fusome suggest it plays novel roles in signaling and transport.
551 317:59–71. doi:10.1016/j.ydbio.2008.02.009.

552 Lin, H., and A.C. Spradling. 1995. Fusome asymmetry and oocyte determination in
553 Drosophila. *Developmental Genetics*. 16:6–12. doi:10.1002/dvg.1020160104.

554 Lin, H., L. Yue, and A.C. Spradling. 1994. The Drosophila fusome, a germline-
555 specific organelle, contains membrane skeletal proteins and functions in cyst
556 formation. *Development*. 120:947–956.

557 Lowe, N., J.S. Rees, J. Roote, E. Ryder, I.M. Armean, G. Johnson, E. Drummond, H.
558 Spriggs, J. Drummond, J.P. Magbanua, H. Naylor, B. Sanson, R. Bastock, S.
559 Huelsmann, V. Trovisco, M. Landgraf, S. Knowles-Barley, J.D. Armstrong, H.
560 White-Cooper, C. Hansen, R.G. Phillips, The UK Drosophila Protein Trap
561 Screening Consortium, K.S. Lilley, S. Russell, and D. St Johnston. 2014.
562 Analysis of the expression patterns, subcellular localisations and interaction
563 partners of Drosophila proteins using a pigP protein trap library. *Development*.
564 141:3994–4005. doi:10.1242/dev.111054.

565 Lu, K., L. Jensen, L. Lei, and Y.M. Yamashita. 2017. Stay Connected: A Germ Cell
566 Strategy. *Trends Genet*. 33:971–978. doi:10.1016/j.tig.2017.09.001.

567 Lu, W., M. Lakonishok, and V.I. Gelfand. 2021. Gatekeeper function for Short stop at
568 the ring canals of the Drosophila ovary. *Current Biology*. 31:3207–3220.e4.
569 doi:10.1016/j.cub.2021.05.010.

570 Maybeck, V., and K. Roper. 2009. A targeted gain-of-function screen identifies genes
571 affecting salivary gland morphogenesis/tubulogenesis in Drosophila. *Genetics*.
572 181:543–565. doi:10.1534/genetics.108.094052.

573 McGough, A., B. Pope, W. Chiu, and A. Weeds. 1997. Cofilin changes the twist of F-
574 actin: implications for actin filament dynamics and cellular function. *The Journal*
575 *of Cell Biology*. 138:771–781. doi:10.1083/jcb.138.4.771.

576 Melak, M., M. Plessner, and R. Grosse. 2017. Actin visualization at a glance. *Journal*
577 *of Cell Science*. 130:525–530. doi:10.1242/jcs.189068.

578 Nashchekin, D., A.R. Fernandes, and D. St Johnston. 2016. Patronin/Shot Cortical
579 Foci Assemble the Noncentrosomal Microtubule Array that Specifies the
580 Drosophila Anterior-Posterior Axis. *Dev Cell*. 38:61–72.
581 doi:10.1016/j.devcel.2016.06.010.

582 Nashchekin, D., L. Busby, M. Jakobs, I. Squires, and D. St Johnston. 2021.
583 Symmetry breaking in the female germline cyst. *Science*. 374:874–879.
584 doi:10.1126/science.abj3125.

585 Niu, W., and A.C. Spradling. 2022. Mouse oocytes develop in cysts with the help of
586 nurse cells. *Cell*. 1–28. doi:10.1016/j.cell.2022.05.001.

587 Oosterheert, W., B.U. Klink, A. Belyy, S. Pospich, and S. Raunser. 2022. Structural
588 basis of actin filament assembly and aging. *Nature*. 1–6. doi:10.1038/s41586-
589 022-05241-8.

590 Pepling, M.E., and A.C. Spradling. 1998. Female mouse germ cells form
591 synchronously dividing cysts. *Development*. 125:3323–3328.

592 Qu, Y., J. Alves-Silva, K. Gupta, I. Hahn, J. Parkin, N. Sanchez-Soriano, and A.
593 Prokop. 2022. Re-evaluating the actin-dependence of spectraplakin functions
594 during axon growth and maintenance. *Dev Neurobiol*. 82:288–307.
595 doi:10.1002/dneu.22873.

596 Rauzi, M., P.-F. Lenne, and T. Lecuit. 2010. Planar polarized actomyosin contractile
597 flows control epithelial junction remodelling. *Nature*. 1–6.
598 doi:10.1038/nature09566.

599 Reynolds, M.J., C. Hachicho, A.G. Carl, R. Gong, and G.M. Alushin. 2022. Bending
600 forces and nucleotide state jointly regulate F-actin structure. *Nature*. 1–7.
601 doi:10.1038/s41586-022-05366-w.

602 Riedl, J., A.H. Crevenna, K. Kessenbrock, J.H. Yu, D. Neukirchen, M. Bista, F.
603 Bradke, D. Jenne, T.A. Holak, Z. Werb, M. Sixt, and R. Wedlich-Soldner. 2008.
604 Lifeact: A versatile marker to visualize F-actin. *Nature Methods*. 5:605–607.
605 doi:10.1038/nmeth.1220.

606 Roper, K., and N.H. Brown. 2004. A spectraplakin is enriched on the fusome and
607 organizes microtubules during oocyte specification in Drosophila. *Curr Biol*.
608 14:99–110.

609 Roper, K., Y. Mao, and N.H. Brown. 2005. Contribution of sequence variation in
610 Drosophila actins to their incorporation into actin-based structures in vivo. *J Cell*
611 *Sci*. 118:3937–3948. doi:10.1242/jcs.02517.

612 Schell, M.J., C. Erneux, and R.F. Irvine. 2001. Inositol 1,4,5-Trisphosphate 3-Kinase
613 A Associates with F-actin and Dendritic Spines via Its N Terminus. *J Biol Chem*.
614 276:37537–37546. doi:10.1074/jbc.M104101200.

615 Spracklen, A.J., T.N. Fagan, K.E. Lovander, and T.L. Tootle. 2014. The pros and
616 cons of common actin labeling tools for visualizing actin dynamics during
617 Drosophila oogenesis. *Developmental Biology*. 393:209–226.
618 doi:10.1016/j.ydbio.2014.06.022.

619 Sun, D., C.L. Leung, and R.K. Liem. 2001. Characterization of the microtubule
620 binding domain of microtubule actin crosslinking factor (MACF): identification of a

621 novel group of microtubule associated proteins. *J Cell Sci*. 114:161–172.
622 doi:10.1242/jcs.114.1.161.

623 Theurkauf, W.E., B.M. Alberts, Y.-N. Jan, and T.A. Jongens. 1993. A central role for
624 microtubules in the differentiation of Drosophila oocytes. *Development*.
625 118:1169–1180.

626 Voelzmann, A., Y.-T. Liew, Y. Qu, I. Hahn, C. Melero, N. S nchez-Soriano, and A.
627 Prokop. 2017. Drosophila Short stop as a paradigm for the role and regulation of
628 spectraplakins. *Seminars in Cell and Developmental Biology*.
629 doi:10.1016/j.semcdb.2017.05.019.

630 Warn, R.M., H.O. Gutzeit, L. Smith, and A. Warn. 1985. F-actin rings are associated
631 with the ring canals of the Drosophila egg chamber. *Exp Cell Res*. 157:355–363.
632 doi:10.1016/0014-4827(85)90120-x.

633 Washington, R.W., and D.A. Knecht. 2008. Actin binding domains direct actin-
634 binding proteins to different cytoskeletal locations. *BMC Cell Biol*. 9:1–16.
635 doi:10.1186/1471-2121-9-10.

636 Wu, X., A. Kodama, and E. Fuchs. 2008. ACF7 regulates cytoskeletal-focal adhesion
637 dynamics and migration and has ATPase activity. *Cell*. 135:137–148.
638 doi:10.1016/j.cell.2008.07.045.

639 Yin, L.-M., M. Schnoor, and C.-D. Jun. 2020. Structural Characteristics, Binding
640 Partners and Related Diseases of the Calponin Homology (CH) Domain.
641 *Frontiers in Cell and Developmental Biology*. 8:342.
642 doi:10.3389/fcell.2020.00342.

643 Yue, J., Y. Zhang, W.G. Liang, X. Gou, P. Lee, H. Liu, W. Lyu, W.-J. Tang, S.-Y.
644 Chen, F. Yang, H. Liang, and X. Wu. 2016. In vivo epidermal migration requires
645 focal adhesion targeting of ACF7. *Nature Communications*. 7:11692.
646 doi:10.1038/ncomms11692.

647 Yue, L., and A.C. Spradling. 1992. hu-li tai shao, a gene required for ring canal
648 formation during Drosophila oogenesis, encodes a homolog of adducin. *Genes*
649 *Dev*. 6:2443–2454.

650

651 **Figure legends**

652

653 **Figure 1. Shot is recruited to the fusome by its actin-binding domain. (A)**
654 Schematic diagram of the *Drosophila* germarium showing germline cyst formation
655 and oocyte specification. **(B)** Diagram of a germline cyst showing how Shot and
656 Patronin translate fusome asymmetry into the polarised MT network that directs
657 dynein transport of oocyte fate determinates into the prospective oocyte (asterisk).
658 Adapted from Nashchekin et al., 2021. **(C)** The domain structure of full-length Shot
659 and Shot truncations. CH, calponin homology domain. ABD, actin-binding domain.
660 **(D-I)** Endogenous Shot **(D)** and ectopically expressed full-length Shot-GFP **(E),** Shot-
661 NC-YFP **(F),** Shot-N-YFP **(G),** Shot ABD-GFP **(H)** localise to the fusome, whereas
662 Shot$^{\Delta ABD}$ **(I)** does not. An enlargement of the fusome is shown on the right. a-
663 Spectrin marks fusome. Phalloidin marks ring canals and the cell cortex. Scale bars,
664 10µm.

665

666 **Figure 2. The Shot CH1 and MT-binding domains are required for the oocyte**
667 **determination. (A-B)** The distribution of Orb in wild type (WT) (**A**) and *shot^{3}* (**B**)
668 germline clone mutant cysts marked by the loss of nlsRFP (blue). **(C)** Shot-N-YFP
669 does not rescue oocyte determination in *shot^{3}* germline clones. **(D)** Expression of
670 Shot NC-YFP in *shot^{3}* mutant cysts restores oocyte specification. **(E-F)** Expression
671 of Shot$^{\Delta CH2}$-GFP **(F)** but not Shot$^{\Delta CH1}$-GFP **(E)** rescues oocyte specification in *shot^{3}*
672 germline clones. Arrows point to the future oocyte; cysts are marked by dashed
673 lines; mutant cysts are labelled by the absence of nuclear RFP (nlsRFP, blue). Scale
674 bars, 10µm.

675

676 **Figure 3. Standard F-actin labelling reagents and CH domain proteins fail to**
677 **recognise fusomal F-actin. (A)** Detection of F-actin on the fusome**.** A confocal
678 image of a germarium stained with anti-actin after heat fixation and post-fixation with
679 fomladehyde (green) and anti-Shot antibody (red). **(B-D)** Localisation of CH domain
680 proteins (green) in cysts stained for a-spectrin (red) to label the fusome and cell
681 cortices and Phalloidin (blue), which labels the ring canals. Utrophin ABD-GFP **(B)**,
682 Filamin-GFP **(C)** and Fimbrin-YFP **(D)** localise to ring canals and the cell cortex but
683 not the fusome. **(E)** A confocal image of a living germarium expressing F-tractin-

684 tdTomato (green) and Shot-YFP (red). Shot localises to the fusome, whereas F-
685 tractin labels the ring canals and cell cortex. **(F-G**) LifeAct does not recognise the
686 fusome. Confocal images of germaria expressing LifeAct-RFP (green) **(F)** and
687 Shot$^{\Delta ABD}$-LifeAct-GFP stained for a-spectrin (red) and Phalloidin (blue) **(G). (H)** A
688 confocal image of a living germarium expressing Shot-YFP (red) and incubated for
689 30 minutes with SiR-actin (green). A weak SiR-actin signal is present on the fusome.
690 The righthand panels show enlargements of the fusome region. Scale bars, 10µm.
691
692 **Figure 4. The Shot CH1 domain recognises the fusome.**
693 **(A-B)** The effects of phosphomimetic Y364D and non-phosphorylatable Y364F
694 mutations. Y364D interferes with Shot ABD localisation to the fusome. Shot-GFP-
695 ABDY364D **(A)** mostly localises to ring canals in region 2b of the germarium. Shot
696 GFP-ABDY364F **(B)** localises like wild-type Shot. **(C-D)** Shot CH1-CH2 localises to
697 the fusome whereas Shot CH1 localises to the fusome and ring canals. Germaria
698 expressing Shot GFP-CH1-CH2 **(C)** and Shot GFP-CH1 **(D)**. **(E)** Shot-NCY364D-
699 YFP mostly localises to ring canals in region 2b of the germarium. **(F)** A germarium
700 expressing ShotY364D-GFP. Mutation of Y364 in full length Shot does not affect
701 Shot localisation. **(G-H)** Deletion of the Shot CH1 domain abolishes binding to the
702 fusome, but CH2 is not required. Germaria expressing Shot$^{\Delta CH1}$-GFP **(G)** and
703 Shot$^{\Delta CH2}$-GFP **(H)**. The righthand panels show enlargements of the fusome region.
704 a-Spectrin (red in the lefthand panels) marks the fusome. Phalloidin (blue) marks the
705 ring canals and cell cortex. Regions of the germarium are indicated on the top. Scale
706 bars, 10µm.
707
708 **Figure S1. (A)** Quantification of fusome and Shot co-localisation in germaria
709 expressing various Shot transgenes and stained with anti-a-Spectrin to label the
710 fusome. Manders' co-localisation coefficient is measured using the JACoP plug-in for
711 Fiji (Bolte and Cordelieres, 2006). Data are means with SD. ****, $P < 0.0001$. **(B)**
712 Ectopically expressed Shot-EF-GAS2-GFP localises to the fusome, whereas Shot C-
713 YFP does not. An enlargement of the fusome is shown on the right. a-Spectrin
714 marks the fusome. Phalloidin marks ring canals and the cell cortex**. (C)** Shot-EF-
715 GAS2-GFP does not localise to the fusome in the absence of endogenous Shot. A
716 germarium expressing Shot-EF-GAS2-GFP (green) in wild type and *shot*^{3} mutant

717 cysts. An enlarged view of the fusome is shown on the right. a-Spectrin (red in left
718 panel) marks the fusome. **(D)** Shot-C-YFP, Shot-EF-GAS2-GFP**,** Shot$^{\Delta ABD}$-GFP and
719 Shot$^{\Delta ABD}$-LifeAct-GFP do not rescue oocyte determination in *shot^{3}* germline clones.
720 Cysts are marked by dashed lines; mutant cysts are labelled by the absence of
721 nuclear RFP (nlsRFP; blue). Scale bars, 10µm.
722
723 **Figure S2. (A)** Actin-42A-GFP localises to the fusome. A germarium expressing
724 Actin-42A-GFP (green) stained with anti-a-Spectrin antibody (red) to mark the
725 fusome. The righthand panel shows an enlarged view of the fusome. **(B)** Fusomal
726 actin is not detected in *hts* mutant cysts. A germarium from a *hts* mutant female
727 stained with anti-Shot (red) and anti-Actin (green) antibodies after heat fixation
728 followed by post-fixation in 8% formaldehyde. **(C)** Diagrams showing the domain
729 structure of actin-binding proteins with calponin homology (CH) domains. ABD, actin-
730 binding domain. **(D)** Live germaria expressing Untrophin ABD-GFP, Filamin-GFP,
731 Fimbrin-YFP and LifeAct-RFP. **(E)** The non-phosphorylatable mutation in Shot
732 Tyr364 does not affect Shot NC and full length Shot localisation. Germaria
733 expressing Shot-NC Y364F-YFP (top) and Shot Y364F-GFP (bottom). The righthand
734 panels show enlargements of the fusome region. a-Spectrin (red in the lefthand
735 panels) marks the fusome. Phalloidin (blue) marks the ring canals and cell cortex.
736 Scale bars, 10µm.
737
738 **Figure S3. Shot localisation in *a-spectrin* and *hts* mutant cysts.** Shot localises to
739 the cell cortex and ring canals in *a-spectrin* **(A)** and *hts* **(B)** mutant cysts, which lack
740 the fusome. **(A)** A germarium with *a-spectrin* germline clones stained with anti-Shot
741 (red), Phalloidin (blue) and anti-b-Spectrin (white) to label the fusome. Mutant cysts
742 are labelled by the absence of nuclear RFP (nlsRFP; blue). *a-spectrin* mutant cysts
743 are marked by dashed lines. Arrows point to the fusome in a wild type cyst. **(B)** A
744 germarium from a *hts* mutant female stained with anti-Shot (red), Phalloidin (blue)
745 and anti-a-Spectrin (red) to label the fusome. Scale bars, 10µm.
746
747 **Video legends**
748
749 **Video 1.** A time-lapse video of Shot-C-YFP in a wild-type germarium. Related to
750 Figure S1B. Images were collected every 1 second on a spinning disc confocal

751 microscope. The video is shown at 15 frames/sec.

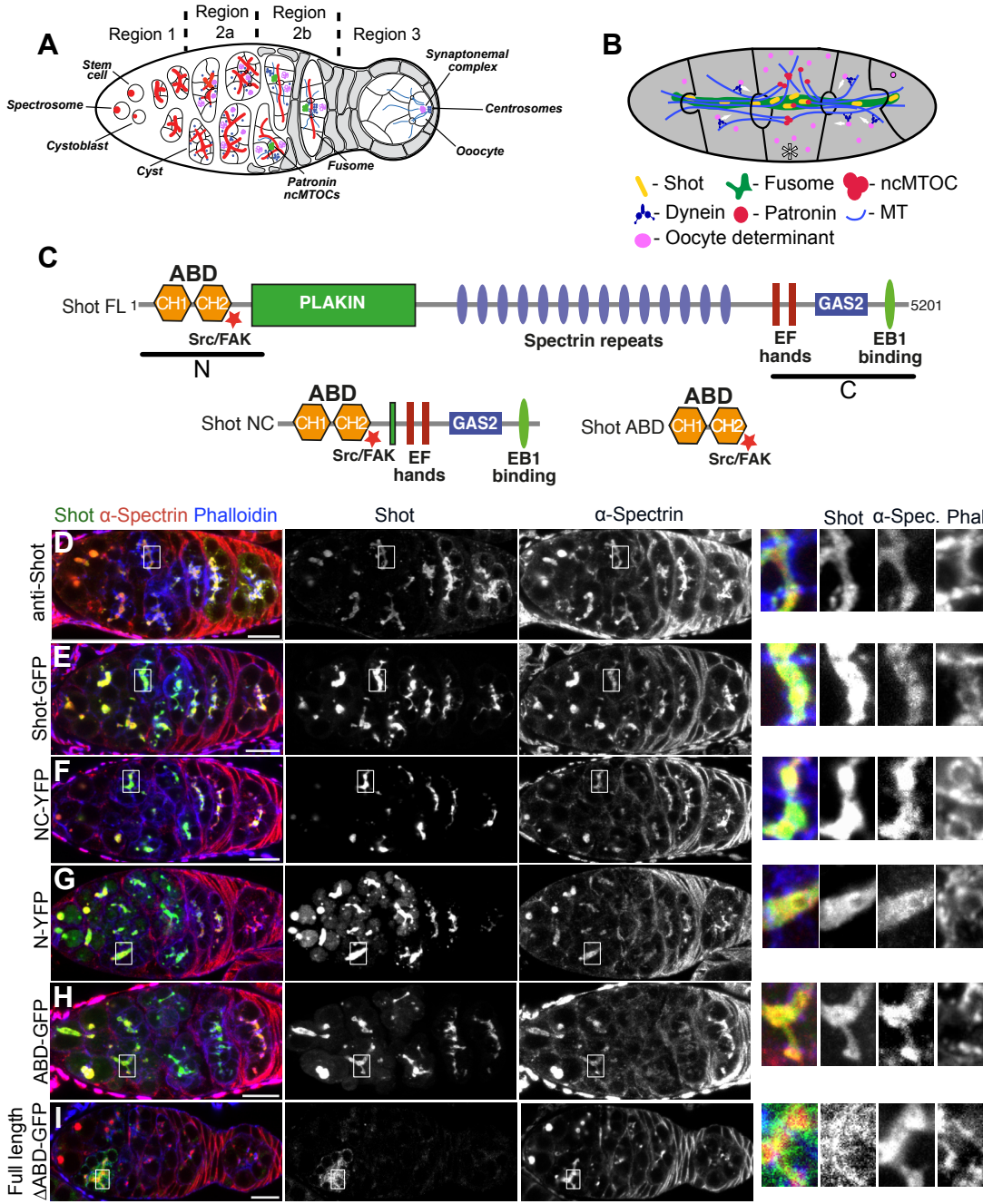

Figure 1. Shot is recruited to the fusome by its actin-binding domain.

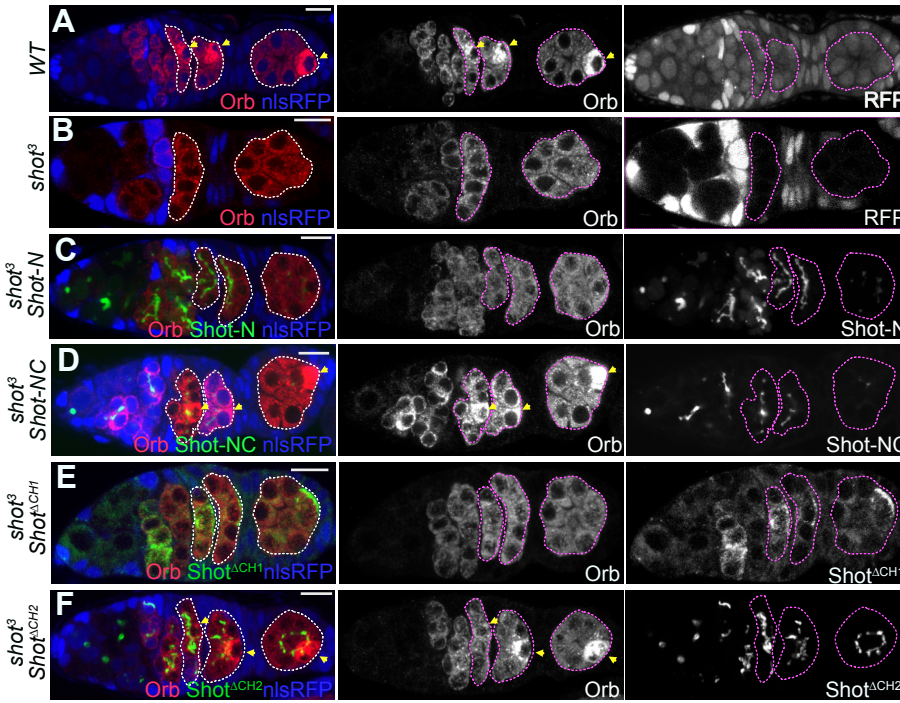

Figure 2. The Shot CH1 and MT-binding domains are required for the oocyte determination

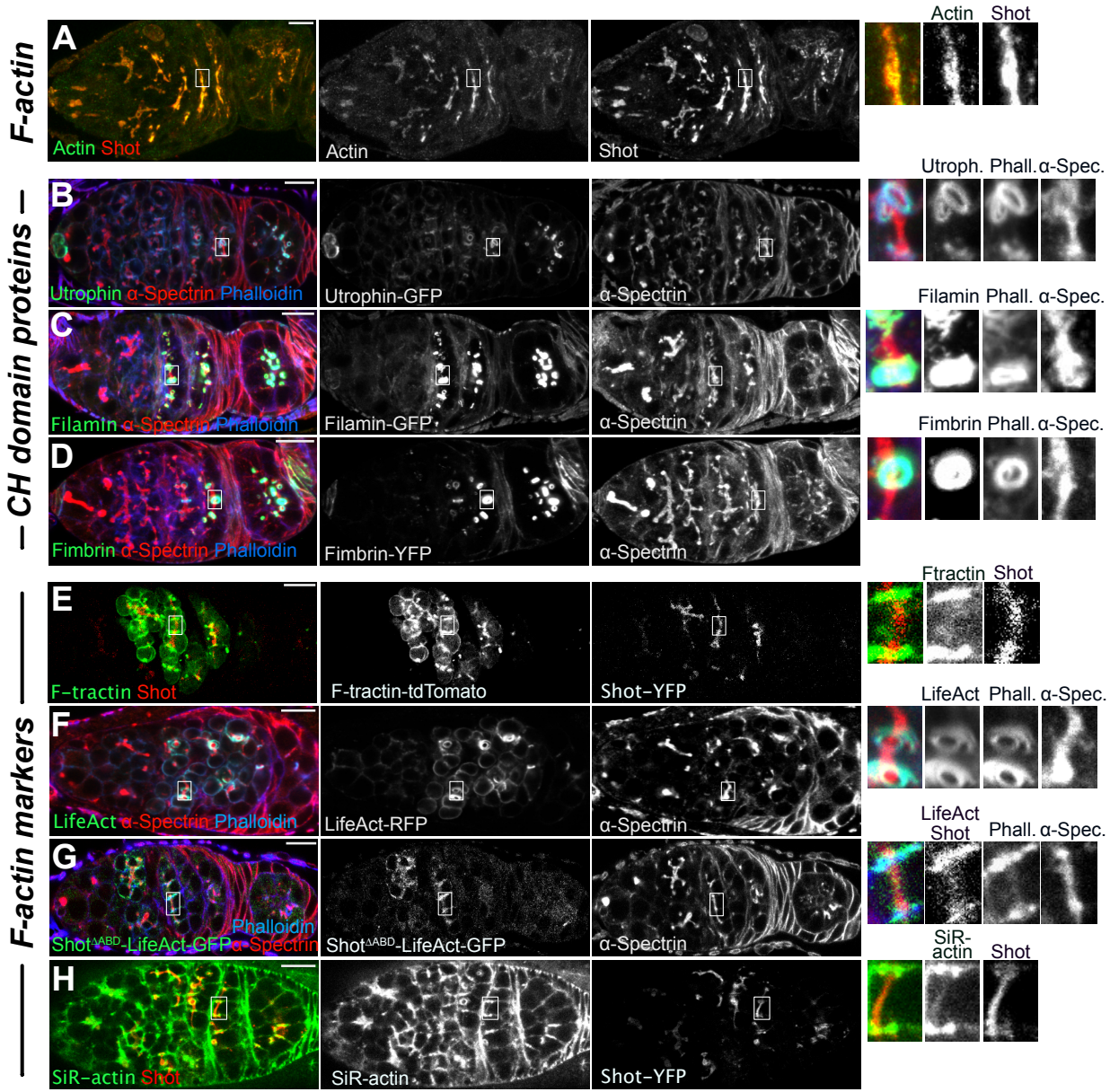

Figure 3. Standard F-actin labelling reagents and some CH domain proteins fail to recognise fusomal F-actin

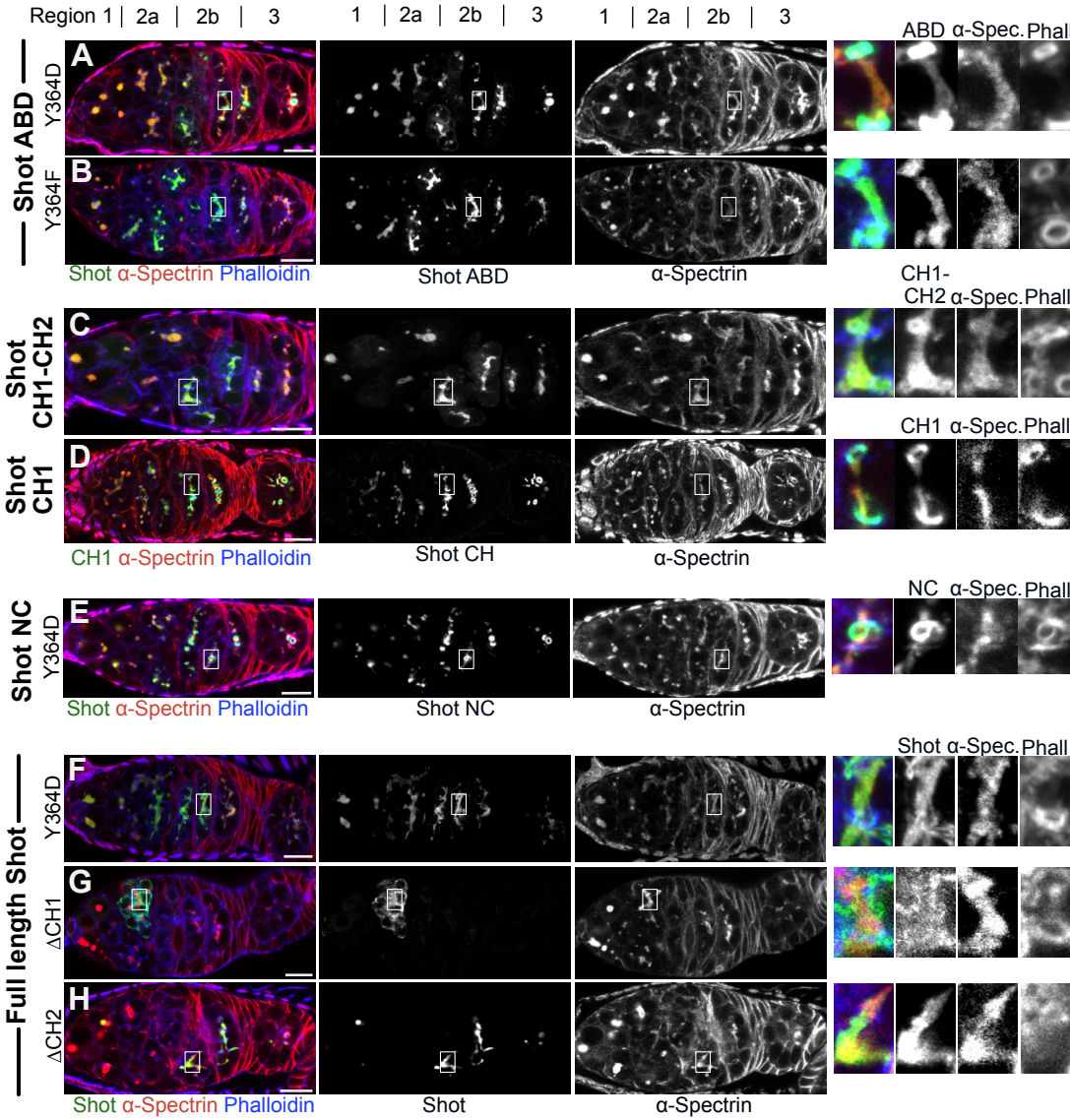

Figure 4. The Shot CH1 domain recognises the fusome

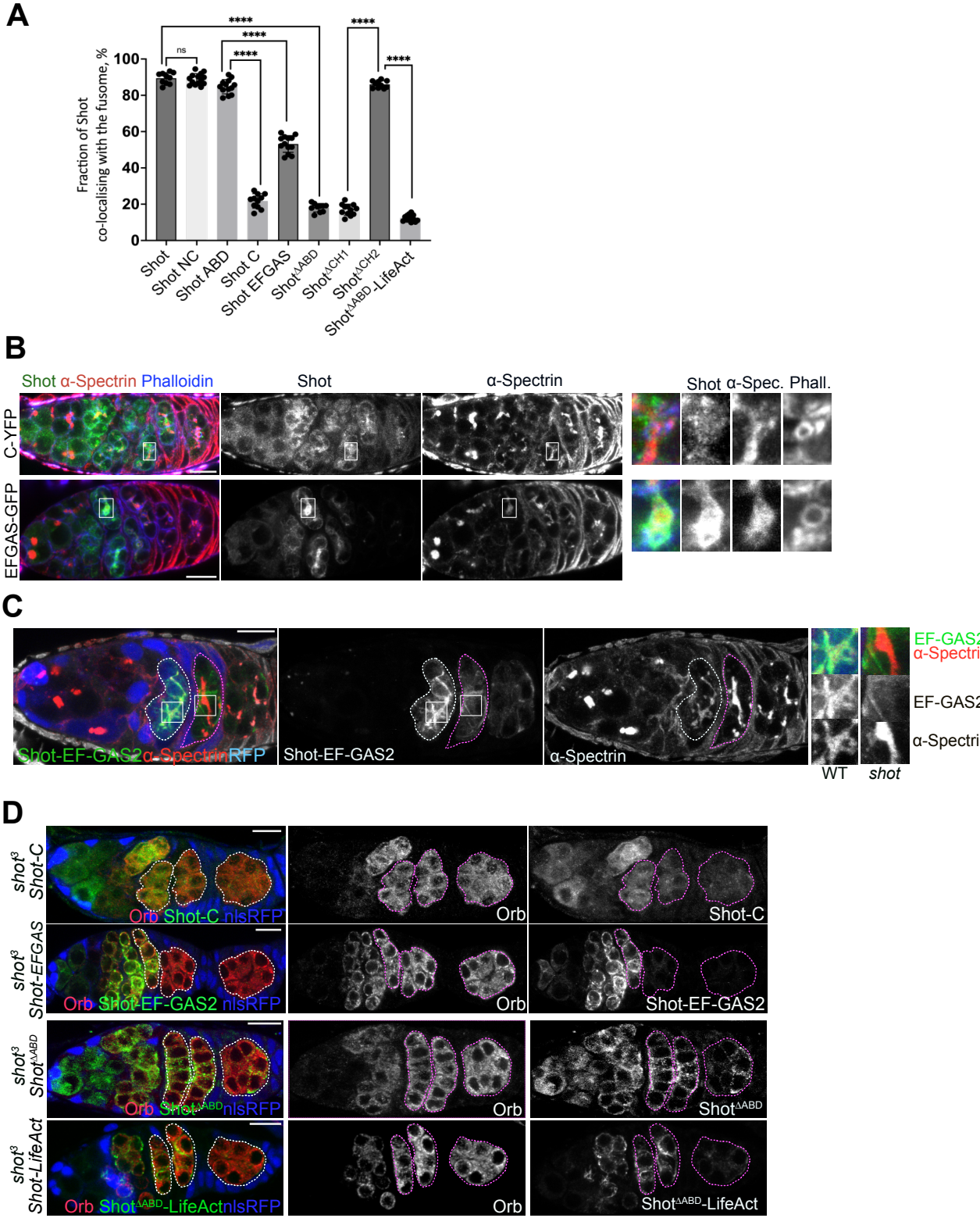
A
Fraction of Shot co-localising with the fusome, %
100
80
60
40
20
0
ns
****
Shot
Shot NC
Shot ABD
Shot C
Shot EFGAS
Shot$^{\Delta ABD}$
Shot$^{\Delta CH1}$
Shot$^{\Delta CH2}$
Shot$^{\Delta ABD}$-LifeAct
B
Shot α-Spectrin Phalloidin
Shot
α-Spectrin
Shot α-Spec. Phall.
C-YFP
EFGAS-GFP
C
Shot-EF-GAS2 α-Spectrin RFP
Shot-EF-GAS2
α-Spectrin
EF-GAS2
α-Spectrin
EF-GAS2
α-Spectrin
WT
shot
D
shot^3 Shot-C
Orb Shot-C nlsRFP
Orb
Shot-C
shot^3 Shot-EFGAS
Orb Shot-EF-GAS2 nlsRFP
Orb
Shot-EF-GAS2
shot^3 Shot$^{\Delta ABD}$
Orb Shot$^{\Delta ABD}$ nlsRFP
Orb
Shot$^{\Delta ABD}$
shot^3 Shot-LifeAct
Orb Shot$^{\Delta ABD}$-LifeAct nlsRFP
Orb
Shot$^{\Delta ABD}$-LifeAct

Figure S1

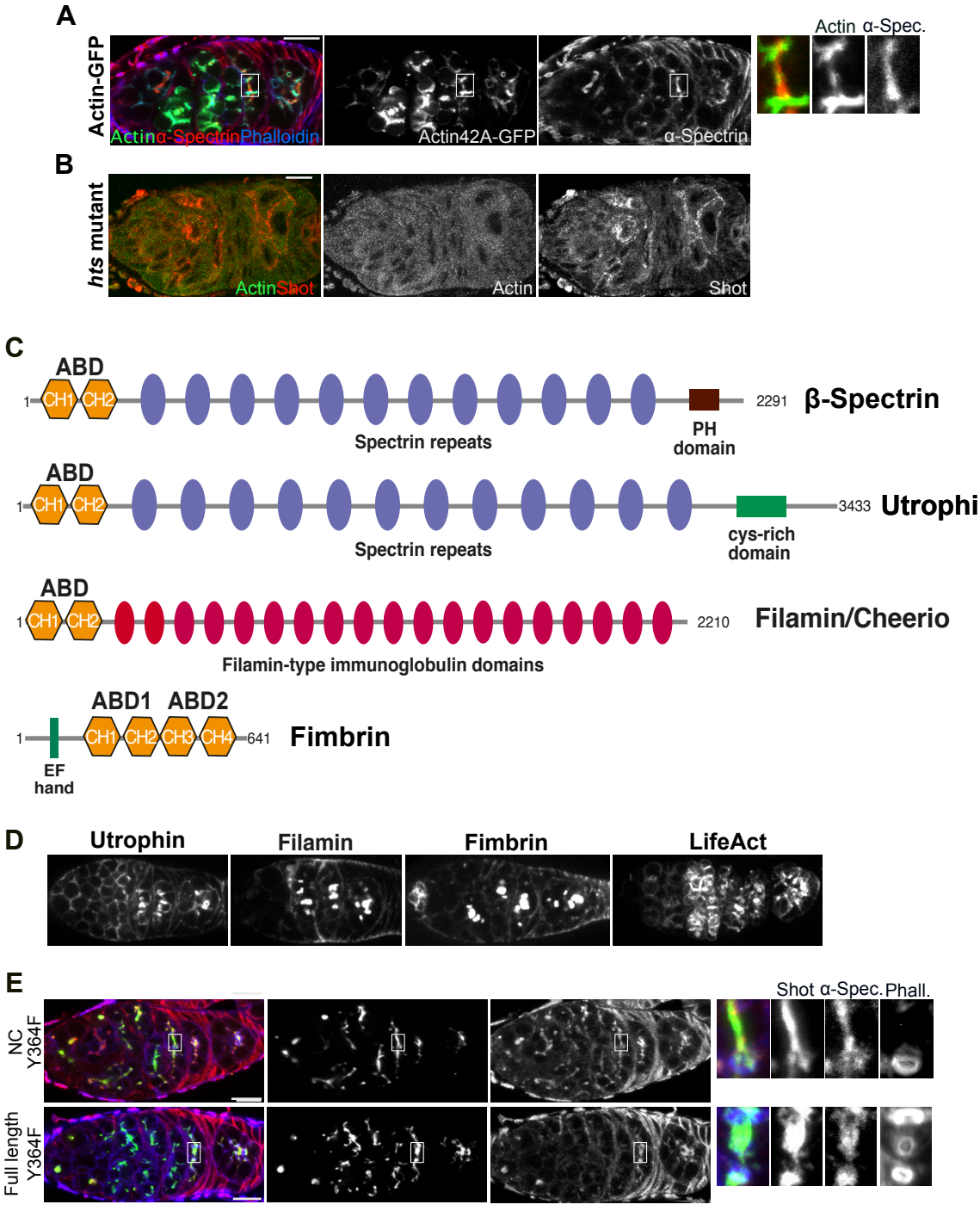
A
Actin-GFP
Actin α-Spectrin Phalloidin
Actin42A-GFP
α-Spectrin
Actin α-Spec.
B
hts mutant
Actin Shot
Actin
Shot
C
ABD
CH1 CH2
1
2291
β-Spectrin
Spectrin repeats
PH domain
ABD
CH1 CH2
1
3433
Utrophin
Spectrin repeats
cys-rich domain
ABD
CH1 CH2
1
2210
Filamin/Cheerio
Filamin-type immunoglobulin domains
ABD1 ABD2
CH1 CH2 CH3 CH4
1
641
Fimbrin
EF hand
D
Utrophin
Filamin
Fimbrin
LifeAct
E
NC Y364F
Full length Y364F
Shot α-Spec. Phall.

Figure S2

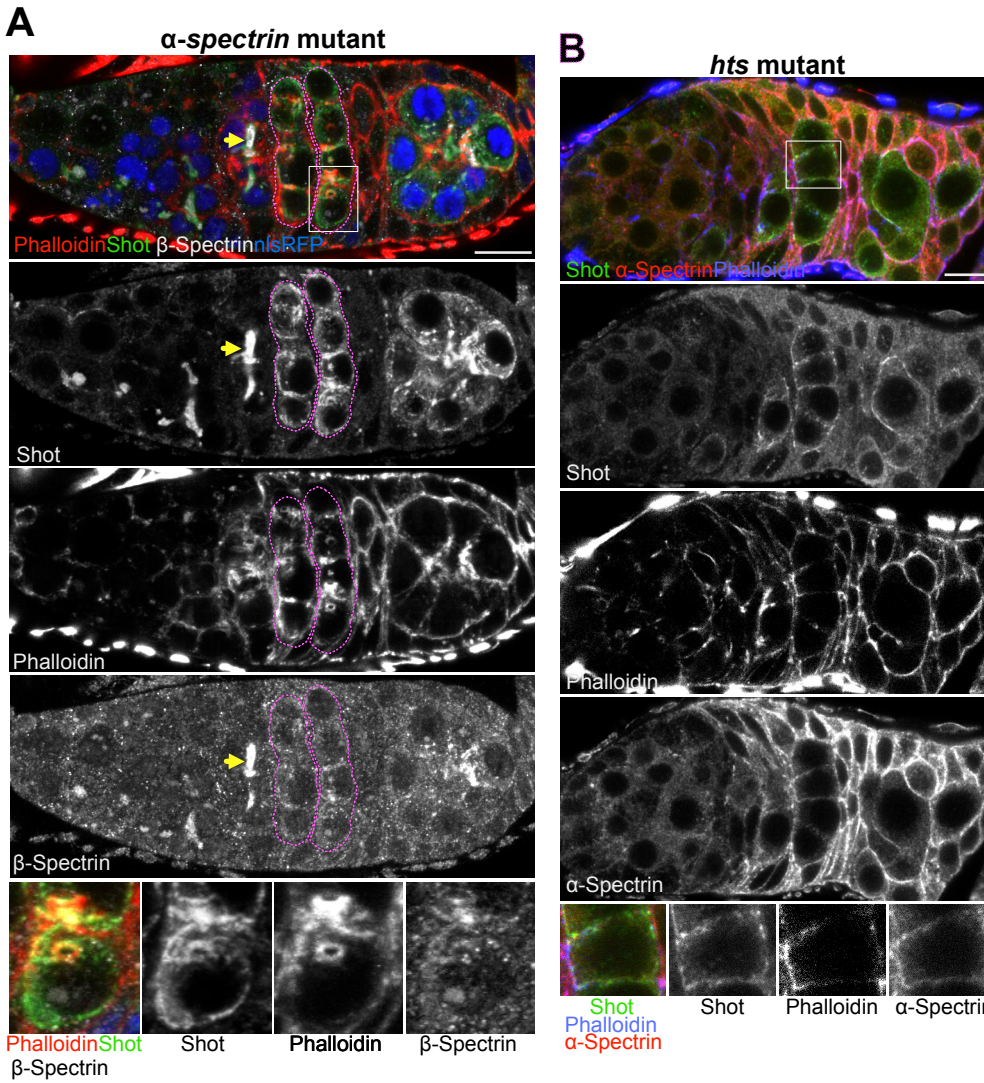

Figure S3. Shot localisation in *α-spectrin* and *hts* mutant cysts

Table S1. Localisation to the fusome and ring canals

Name of the protein	Localisation to the fusome / number of cysts analysed	Localisation to ring canals / number of cysts analysed	Number of germaria analysed
Shot FL	63/63	0/63	11
Shot NC	71/71	0/71	10
Shot N	66/66	0/66	10
Shot C	0/42	0/42	10
Shot EF-GAS2	32/32	0/32	8
Shot ABD	58/58	0/58	10
Shot$^{\Delta ABD}$	0/34	0/34	16
Shot$^{\Delta ABD}$-LifeAct*	0/41	5 /41	12
Shot$^{\Delta CH1}$	0/31	0/31	10
Shot$^{\Delta CH2}$	47/47	0/47	10
Shot Y364D	74/74	0/40 (region 2a) 0/34 (region 2b)	10
Shot Y364F	45/45	0/25 (region 2a) 0/20 (region 2b)	10
Shot NC Y364D	49/49	10/27(region 2a) 22/22(region 2b)	10
Shot NC Y364F	45/45	0/24 (region 2a) 0/21(region2b)	10
Shot ABD Y364D	55/55	14/31(region 2a) 24/24(region2b)	10
Shot ABD Y364F	53/53	0/28 (region 2a) 0/25 (region 2b)	10
Shot CH1	53/53	13/29 (region 2a) 24/24 (region 2b)	10
Utrophin ABD	0/50	50/50	10
Filamin	0/51	51/51	10
Fimbrin	0/42	42/42	10
F-tractin	0/49	49/49	12
LifeAct	0/42	42/42	8
SiR-actin	41/41	41/41	8